G protein-coupled receptors sense fluid shear stress in endothelial cells

Mirianas Chachisvilis†, Yan-Liang Zhang, and John A. Frangos

La Jolla Bioengineering Institute, 505 Coast Boulevard South, La Jolla, CA 92037

Communicated by Peter M. Rentzepis, University of California, Irvine, CA, August 23, 2006 (received for review April 18, 2006)

Hemodynamic shear stress stimulates a number of intracellular events that both regulate vessel structure and influence development of vascular pathologies. The precise molecular mechanisms by which endothelial cells transduce this mechanical stimulus into intracellular biochemical response have not been established. Here, we show that mechanical perturbation of the plasma membrane leads to ligand-independent conformational transitions in a G protein-coupled receptor (GPCR). By using time-resolved fluorescence microscopy and GPCR conformation-sensitive FRET we found that stimulation of endothelial cells with fluid shear stress, hypotonic stress, or membrane fluidizing agent leads to a significant increase in activity of bradykinin B_2 GPCR in endothelial cells. The GPCR conformational dynamics was detected by monitoring redistribution of GPCRs between inactive and active conformations in a single endothelial cell under fluid shear stress in real time. We show that this response can be blocked by a B_2-selective antagonist. Our data demonstrate that changes in cell membrane tension and membrane fluidity affect conformational dynamics of GPCRs. Therefore, we suggest that GPCRs are involved in mediating primary mechanochemical signal transduction in endothelial cells. We anticipate our experiments to be a starting point for more sophisticated studies of the effects of changes in lipid bilayer environment on GPCR conformational dynamics. Furthermore, because GPCRs are a major target of drug development, a detailed characterization of mechanochemical signaling via the GPCR pathway will be relevant for the development of new antiatherosclerosis drugs.

conformational transition | ligand-independent activation | mechanochemical signal transduction | plasma membrane | bradykinin

A major challenge is identification of the mechanisms by which mechanical forces are converted into a sequence of intracellular biochemical signals in endothelial cells. A number of mechanosensitive biological molecules have been identified, including mechanically gated channels (1), receptors (2), G proteins (3), enzymes (4), and cytoskeleton. Numerous studies have demonstrated that mechanochemical signal transduction originates at the cell membrane (1, 3, 5). Experiments on purified heterotrimeric G proteins reconstituted into liposomes have shown that, even in the absence of any other potential mechanosensors, the G proteins are activated by fluid shear stress (3). This finding suggests that the lipid bilayer membrane itself plays a major role in mediating mechanochemical signal transduction, which would be expected considering the importance of lipid–protein interactions for function of membrane proteins (6). Recently, it has been reported that mechanical stretching of cells can activate angiotensin II type 1 G protein-coupled receptor (GPCR) (7). However, this study did not completely rule out possible contributions from a ligand-dependent intracrine pathway; it has been shown that autocrine release of angiotensin II does mediate the stretch-induced response (8). Typically the activity of GPCRs is initiated when an extracellular ligand induces or binds to an active conformation (9). Information regarding conformational changes involved in GPCR activation is mostly derived from biophysical studies on rhodopsin (10), β_2-adrenergic (11, 12), α_{2A} adrenergic (13), parathyroid hormone (13), and adenosine receptors (14). It has been shown that certain key amino acid residues in transmembrane helices, interacting with each other, keep the receptor preferentially locked in an inactive state. Ligand binding or isomerization of the preloaded ligand retinal (in rhodopsin) causes movement of helices 5, 6, and 7, resulting in a conformational change responsible for activation of G proteins (9). It has been shown that GPCR structure is rather "plastic," i.e., the GPCR can assume a number of different conformations depending on the specific ligand (9, 11, 15). Because the lipid bilayer makes up the core structure of the cell membrane by creating a 2D solvent within which membrane-associated signaling molecules interact and function it is expected that any change in the physical properties of the bilayer can have a strong effect on signaling dynamics (6).

To test the hypothesis that mechanical forces initiate mechanochemical signal transduction by increasing membrane tension and altering physical properties of the cell membrane, we have chosen to study human B_2 bradykinin GPCR, which is known to be involved in a fluid flow-dependent response in endothelial cells (16–18). Here, we demonstrate that the B_2 receptor changes conformation when stimulated by fluid shear stress, hypotonic shock, and benzyl alcohol in the absence of any ligand.

Results

Detection and Characterization of Ligand-Induced GPCR Conformational Change. To monitor conformational dynamics of the GPCR, we constructed a B_2 receptor chameleon (B2K) with yellow fluorescent protein (YFP) inserted into the third cytoplasmic loop and cyan fluorescent protein (CFP) fused to the C terminus similarly as reported earlier for adrenergic (α_{2A}), parathyroid hormone, and adenosine receptors (13, 14) (see Fig. 1*a Inset*). The B2K chameleon expressed in bovine aortic endothelial cells (BAECs) displays mostly membrane localization (Fig. 1*b*) and a dual fluorescence spectrum with characteristic CFP and YFP emission peaks at ≈485 and 525 nm, respectively. We have estimated the FRET transfer efficiency in an unactivated B2K chameleon from YFP photobleaching-induced changes in isotropic fluorescence decay kinetics of donor (CFP) emission at 483 nm; upon photobleaching of the acceptor (YFP) the average lifetime of CFP emission increased from 1.51 ± 0.018 to 1.70 ± 0.019 ns, implying FRET efficiency of ≈11% (data not shown; note that CFP emission kinetics were fitted to a multiexponential decay model containing three exponential decay components from which the average lifetimes were calculated).

Fig. 1*a* shows that exposure of BAECs expressing B2K chameleon to their natural agonist bradykinin results in a pronounced

Author contributions: M.C. and Y.-L.Z. designed research; M.C. and Y.-L.Z. performed research; M.C., Y.-L.Z., and J.A.F. analyzed data; and M.C. wrote the paper.

The authors declare no conflict of interest.

Abbreviations: GPCR, G protein-coupled receptor; YFP, yellow fluorescent protein; EYFP, enhanced YFP; CFP, cyan fluorescent protein; ECFP, enhanced CFP; BAEC, bovine aortic endothelial cell.

†To whom correspondence should be addressed. E-mail: mirianas@ljbi.org.

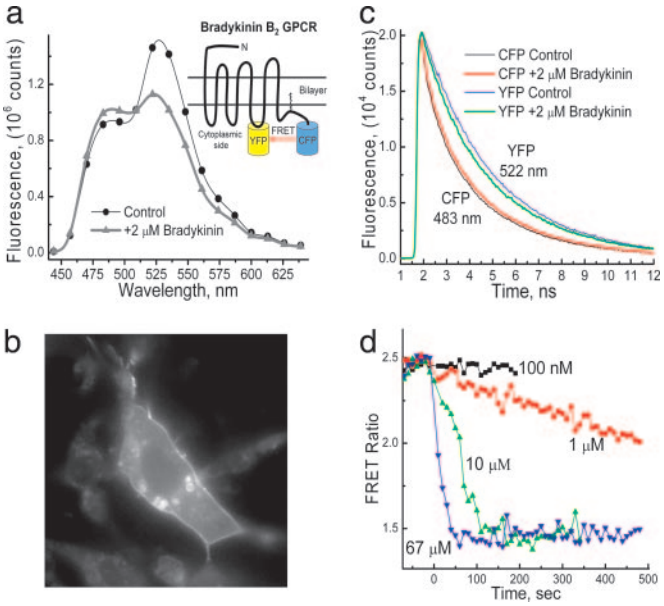

Fig. 1. Detection of B_2 conformational change. (*a*) Integrated polarized fluorescence spectra of B2K chameleon in a single BAEC before and after stimulation with bradykinin. (*b*) Fluorescence microscopy image of BAECs expressing B2K chameleon. Image was taken through a CFP filter. (Magnification: × 650.) (*c*) Polarized fluorescence decay kinetics of B2K chameleon from a single BAEC before and after stimulation with agonist. (*d*) Response of FRET ratio of B2K chameleon in a BAEC to stimulation by different concentrations of bradykinin at $t = 0$.

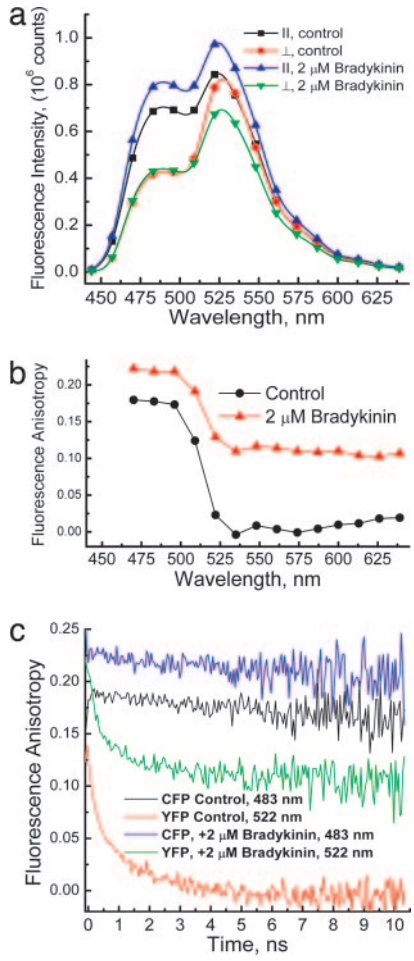

Fig. 2. Agonist-induced changes in fluorescence anisotropy. (*a*) Parallel and perpendicular components of integrated fluorescence spectrum of B2K chameleon in a BAEC before and after stimulation with bradykinin. (*b*) Fluorescence anisotropy spectra of B2K chameleon in a BAEC before and after stimulation with agonist. (*c*) Time-resolved emission anisotropy of B2K chameleon in a single BAEC before and after exposure to agonist. Transient anisotropy traces are shown at both CFP and YFP emission wavelengths. The fast decay of the YFP anisotropy (decay constant ≈1 ns) is a direct manifestation of the FRET process from CFP.

spectral change characterized by a decrease in YFP emission and an increase in CFP emission; corresponding fluorescence emission kinetics show that the fluorescence decay of CFP becomes slower, whereas fluorescence decay of YFP becomes faster (Fig. 1*c*), suggesting that conformational change leads to lower FRET efficiency. These changes are completely reversible upon washing off the ligand. The time scale of the ligand-induced GPCR response depends on the ligand concentration; the data in Fig. 1*d* show the ligand concentration-dependent effect on FRET ratio (ratio of YFP emission intensity at ≈525 nm to CFP emission intensity at ≈485 nm). Note that the IC_{50} for the B2K chameleon (Fig. 5**,** which is published as supporting information on the PNAS web site) is significantly shifted to higher concentrations compared with the IC_{50} of native B_2 (≤ 1 nM) (19–21); this shift is caused by the effects of the insertion of fluorescing proteins and was also observed earlier in the case of parathyroid hormone and α_{2A} adrenergic receptor chameleons as a decrease in binding affinity and increase in the IC_{50} (13). We have detected no change in FRET of B2K chameleon caused by exposure to B_2-selective antagonist HOE140 (10 μM), suggesting that constitutive activity of B2K is low.

To characterize the nature of the B2K conformational change we have recorded polarized fluorescence intensity and anisotropy spectra (Fig. 2). Fig. 2*a* shows that ligand response of parallel and perpendicular fluorescence components are rather different: whereas the change in the spectrum of the parallel component is minimal, the spectrum of the perpendicular component exhibits a significant decrease in the ratio of YFP-to-CFP emission intensities; these data were used to calculate fluorescence anisotropy spectra that are presented in Fig. 2*b*. The first important observation is that anisotropy of CFP emission increases upon ligand stimulation. Because change in FRET efficiency should not have any significant effect on CFP emission anisotropy (which is nearly constant during the lifetime of CFP emission; see Fig. 2*c*) we assign this increase in anisotropy to the ligand-induced rotation of C terminus in such a way that the transition dipole moment of the attached CFP molecule becomes more parallel to the plane of the plasma membrane. Note that our measurements are done on BAECs that are virtually flat when adhered to the substrate (22); therefore the orientation of the majority of GPCRs is fixed within the plane of the plasma membrane, which is mostly parallel to the glass substrate. The fact that the initial anisotropy of CFP emission (≈0.19, see Fig. 2 *b* and *c*) is lower than the expected value of ≈0.3 (see *Methods*) confirms that the orientation of CFP is fixed with respect to the plane of plasma membrane. The second observation is that anisotropy of YFP emission increases upon ligand stimulation (Fig. 2 *b* and *c*). This increase is caused by multiple factors. First, the relative contribution of FRET-depolarized YFP emission becomes smaller compared with directly excited CFP and YFP emissions [which are highly polarized (23)] in the wavelength range of ≈525 nm. Second, the fact that the parallel component of YFP emission increases upon ligand stimulation despite the net decrease in FRET efficiency [which was established by comparing isotropic (magic angle) emission spectra constructed from fluorescence component spectra shown in Fig. 2*a*] suggests that conformational change not only results in a larger distance between CFP and YFP but also a change in relative orientation of CFP and YFP, which leads to a more parallel alignment of their transition dipole moments in a ligand-

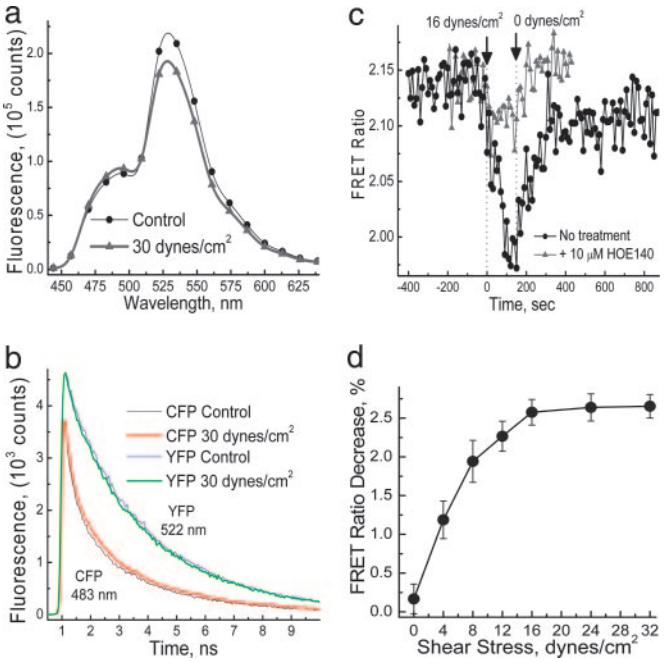

Fig. 3. Response of B_2 GPCR to fluid shear stress. (*a*) Integrated polarized fluorescence spectra of B2K chameleon in a single BAEC before and after stimulation with fluid shear stress for 2 min. (*b*) Response of fluorescence decay kinetics of B2K chameleon to stimulation by shear stress for 2 min. (*c*) Response of FRET ratio of B2K chameleon in a BAEC exposed to shear stress in the absence and presence of selective B_2 antagonist. Flow is turned on at time $t = 0$ and off at $t = 150$ s. (*d*) Fluid shear stress induced change in FRET ratio of B2K chameleon in a BAEC as a function of shear stress magnitude.

bound conformation. The decrease in FRET efficiency caused by the larger distance between donor and acceptor is more significant than the increase in FRET efficiency because of more parallel alignment of transition dipole moments in the activated state of the GPCR. These data indicate that the B2K is functional in terms of ligand binding and the nature of structural change in the B2K is rather different from the α_{2A} receptor for which no change in anisotropy has been reported under similar experimental conditions (12).

It should be noted that the FRET ratio of B2K chameleons expressed in BAECs varies by ≈20% from cell to cell; this variation is caused by a small fraction of B2Ks localized in the cytoplasmic organelles that exhibit nearly zero FRET efficiency, indicating improper folding. Cells that exhibit mostly plasma membrane localization have higher FRET ratios, suggesting that B2Ks in the membrane are in a properly folded inactive conformational state.

Fluid Shear Stress Induced GPCR Conformational Changes. To test the hypothesis that changes in membrane physical properties can lead to GPCR conformational change required for activation, we studied the effect of fluid shear stress on B2K chameleon expressed in endothelial cells. Fig. 3*a* shows that when BAECs expressing B2K chameleon are exposed to fluid shear stress of 30 dynes/cm^2 for 2 min a similar spectral change results as in the case of ligand binding (compare with Fig. 1*a*). The time-resolved fluorescence decay kinetics presented in Fig. 3*b* also show that the fluorescence decay of CFP becomes slower, whereas fluorescence decay of YFP becomes faster, suggesting that shear stress leads to conformational change, which manifests itself as a decrease in FRET ratio by up to 8%. To test the kinetics of GPCR conformational change we measured the response of B2K in a single cell to a square impulse of fluid shear stress (rise time <200 ms) applied at time 0 and turned off after 150 s (Fig. 3*c*); data show that there is a rapid decrease in FRET with the time constant of ≈80 s followed by slower recovery after fluid shear stress is turned off. We tentatively interpret this response as shear stress-induced GPCR conformational change caused by increased plasma membrane tension. The polarization properties of the shear stress-induced changes were similar as reported above for ligand-induced response. When the same experiment was done in the presence of B_2-selective antagonist HOE140, the shear stress response was significantly inhibited. Note that an IC_{50} that is at least 100–1,000 times lower for ligand-induced response of B2K chameleon (compared with native B_2 receptor, see dose–response of FRET ratio in Fig. 5) makes it rather unlikely that this conformational change is caused by an autocrine pathway (17). Endothelial cells are known to secrete tissue kallikreinin, which remains at the cell membrane and regulates conversion of kininogen into lys-bradykinin, which is equally potent as bradykinin. In the presence of 20 μM aprotinin no statistically significant inhibition of fluid shear stress response was observed in our experiments; the shear stress-induced FRET decrease was 4.7 ± 0.6% in the absence and 6.9 ± 1.2% in the presence of aprotinin (*t* test resulted in $P = 0.185$, sample size 12 cells). This result further confirms that an autocrine activation pathway is not involved in the shear-induced B2K conformational change.

In Fig. 3*d* we show the B2K FRET ratio response as a function of fluid shear stress magnitude. These data indicate that the fraction of GPCRs or the degree of conformational change of all GPCRs undergoing conformational change saturates at physiological shear stress values (≈15 dynes/cm^2).

GPCR Conformational Transitions Caused by Hypotonic Membrane Stretch. As in the case of shear stress, exposure of a cell expressing B2K chameleon to hypotonic medium (osmolality change from 284 to 142 mOsm/kg) leads to a reversible decrease of FRET ratio signal by ≈10%, indicating a conformational change (Fig. 4 *a* and *b*). We believe this change is caused by osmotic water influx into the cell and the accompanying increase in the cell membrane tension. The time scale of the response to hypotonic shock (≈15 min) is slower than in the case of shear stress stimulation (see Fig. 4*a Inset*), most likely because the active osmoregulation by the endothelial cell is resisting water influx through the membrane. The observed FRET change can be reversed by restoring osmolality back to 284 mOsm/kg.

Effect of Membrane Fluidity Enhancers on GPCR Conformational Equilibrium. To further investigate the potential mechanisms of flow-induced GPCR activation, plasma membrane fluidity of BAECs was increased with benzyl alcohol, a known membrane fluidity enhancer, which acts by increasing membrane free volume. The data shown in Fig. 4*c* indicate that the presence of benzyl alcohol in the cell membrane also leads to conformational change of the B2K on the time scale of ≈180 s. To determine the partitioning time of the benzyl alcohol into cell's membrane we used the lipid-like molecular rotor KW-04, whose fluorescence quantum yield is sensitive to viscosity of the environment (Fig. 4*d*); its fluorescing properties are similar to related molecular rotors used to measure membrane microviscosity (24, 25). Molecular rotors of this type exhibit viscosity-dependent fluorescence quantum yield caused by the radiationless deactivation process via intramolecular rotational motion and therefore can be used as membrane fluidity probes. Note that KW-04, which partitions almost exclusively into the cell membrane (see Fig. 6, which is published as supporting information on the PNAS web site), is sensitive to benzyl alcohol-induced changes in the plasma membrane only (fluorescence quantum yield of KW-04 decreases at lower viscosities). Fig. 4*d* shows that the fluorescence intensity of KW-04 decreases rapidly when cells stained with

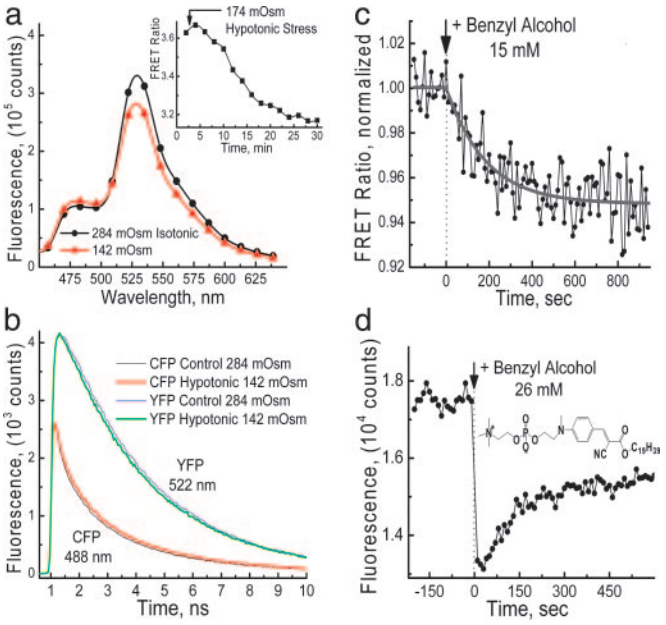

Fig. 4. Response of B_2 GPCR to hypotonic shock (*a* and *b*) and the membrane fluidizing agent benzyl alcohol (*c* and *d*). (*a*) Changes in integrated polarized fluorescence spectra of B2K chameleon in a single BAEC caused by stimulation by hypotonic shock for 15 min. (*Inset*) Time-dependent response of FRET ratio caused by hypotonic shock. (*b*) Polarized fluorescence decay kinetics of B2K chameleon from a BAEC before and after stimulation with hypotonic medium for 15 min. Increase in a fluorescence lifetime of the donor (CFP) and decrease in a fluorescence lifetime of the acceptor (YFP) are clearly visible. (*c*) The dynamics of FRET ratio of B2K chameleon in a BAEC exposed to benzyl alcohol at time $t = 0$. Gray line shows a fit with a monoexponential rise function with a time constant of 180 s. (*d*) Integrated fluorescence signal from a BAEC stained with molecular rotor KW-04 and exposed to benzyl alcohol at time $t = 0$.

KW-04 are exposed to benzyl alcohol, indicating that partitioning of benzyl alcohol into plasma membrane is complete within 10 s. Therefore the observed 180-s response time of B2K chameleon can be attributed to changes in the GPCR conformational equilibrium induced by modulation of plasma membrane fluidity by benzyl alcohol.

Discussion

The GPCR superfamily includes several thousand receptors that respond to extracellular signals as diverse as photons, odorants, tastants, nucleotides, peptides, and ions. Many GPCRs also exhibit agonist-independent constitutive activity, suggesting that GPCRs can adopt active conformation spontaneously (9, 26). Therefore, it seems clear that there is no common mechanism for activating GPCRs (9, 15). However, it is quite well established that the activity of integral membrane proteins is significantly affected by interactions with the lipid molecules (6). Several lines of reasoning support our hypothesis that the observed changes in conformational equilibrium of B_2 GPCR (Figs. 3 and 4 *a* and *b*) are caused by modulation of plasma membrane properties by membrane tension.

In a simplified equilibrium model, a GPCR protein isomerizes between two different states, an inactive R and an active R* conformation, which differ in their ability to catalyze G protein activation (26); because of structural constraints the equilibrium lies toward the inactive R state. However, there is a growing understanding that the equilibrium model cannot adequately describe a number of experimental observations and therefore has to be replaced by nonequilibrium models (27, 28). The key difference between equilibrium and nonequilibrium models relevant to this work is that mechanically induced changes in physical properties of membrane environment will affect differently the distribution between R and R* states. Those membrane microenvironment changes that affect conformational reaction rates can only change the distribution between R and R* states in the nonequilibrium model (see below). In contrast, other types of environmental changes discussed below affect relative energies of R and R* conformations, leading to preferential stabilization of one conformation; in this case both models predict a change in conformational equilibrium. Below we discuss which physical properties of the plasma membrane can change under mechanical perturbation and which of these changes can lead to a shift in conformational equilibrium of B_2 GPCR.

The lipid bilayer is a unique composite dynamic structure held together by an exact balance of hydrophobic and lipid–lipid interactions. Because of the high degree of spatial inhomegeneity, the interior of the lipid bilayer is characterized by strong lateral pressure forces that vary greatly with the depth within the bilayer. Molecular dynamics calculations show that when a membrane is stretched by an external force the steric repulsive interactions are reduced, whereas interfacial tension is increased because of increased exposure of hydrophobic tails of the lipids to water, leading to an overall change in lateral pressure profile (29). It has been suggested that these changes in intrabilayer pressure profiles are responsible for activation of certain membrane proteins such as gated membrane channels (29). Increasing membrane tension beyond 0.5 dynes/cm leads to a linear regime where an increase in tension results in linear area expansion (30). Accompanying the lateral stretching, the thickness of the bilayer decreases because of weak coupling between the area and the volume. When the bilayer is stretched isotropicaly the lipids become more loosely packed, whereas lipid tails become more disordered (29). In contrast, a recent theoretical study showed that when lipid bilayer is exposed to flow shear stress the orientational order of lipids increases substantially (31); not only is this expected to result in significant changes in lateral pressure profile but lateral membrane viscosity is likely to be affected because flow induces noticeable changes in bilayer membrane density profiles (31). A change in bilayer thickness is a factor that affects both the lateral pressure profile and the hydrophobic matching (6) between hydrophobic parts of the lipid bilayer and the membrane protein. If the hydrophobic thickness of a membrane protein is smaller in one of the conformational states of the GPCR then a decrease in bilayer thickness would shift equilibrium toward that conformation (6). In this case the enrichment of R* conformation is caused by a decrease of its free energy and can be explained within the equilibrium model. There are many examples that hydrophobic membrane thickness controls functioning of membrane proteins such as gramicidin *A* ion channel (32), cytochrome *c* oxidase, and Ca^{2+}-ATPase or (Na^{+}-K^{+}) ATPase. Particularly important is the example of rhodopsin, which is known to be very sensitive to its lipid environment and can be made functional in an artificial membrane without any of the lipids native to its natural environment by making a membrane with the correct balance of pressures in the lipid headgroup and tail regions (33, 34). The precise information about GPCR structural changes caused by conformational transition is lacking. Previous studies on bacteriorhodopsin and β_2 adrenergic receptor suggest that receptor activation is accompanied by tilting and rotation of transmembrane helices 6 and 3 (9, 35, 36), which is consistent with our anisotropy data (Fig. 2). Tilting of the transmembrane helix would result in reduction of hydrophobic thickness of R* conformation, thus stabilizing this conformation upon thinning of the bilayer. Therefore in principle the observed change in conformational equilibrium of B2K receptor (Fig. 3) can be attributed to a change in membrane thickness and potentially higher level of hydration of the bilayer under mechanical tension (37).

The lateral fluidity of the lipid bilayer membrane is considered to be one of the key functions of the cell membrane by enabling lateral diffusion, interactions, and signaling by various mem-

brane-associated signaling proteins. It has been reported that fluid shear stress increases fluidity of endothelial cell membrane (24, 38). A change in membrane fluidity cannot directly change the equilibrium distribution between conformational states of a GPCR because this change should affect both forward and back reaction rates equally (6). However, membrane fluidity can have significant effect if the initial distribution is not an equilibrium one, which is the case in a live cell caused by GPCR participation in metabolically driven G protein catalysis cycle. According to the Kramers reaction rate theory (39) reaction rate is inversely proportional to viscosity:

$$k_{\text{act}} \propto \frac{1}{\eta} e^{-\Delta H/RT}, \qquad [1]$$

where ΔH is activation energy. This equation states that a decrease in membrane microviscosity has the same effect on reaction rate as lowering overall reaction barrier; thus, it is similar in action to a catalyst. Our experiments with the membrane fluidizing agent benzyl alcohol (Fig. 4*c*) indicate that indeed a higher membrane fluidity shifts conformational equilibrium toward the R* conformation. Therefore it is feasible that change in membrane fluidity can explain the observed conformational changes in B2K GPCR. Note that enhanced membrane lateral fluidity has also been reported for liposomes and protoplasts under hypoosmotic stress (40), which can explain the observed B2K conformational dynamics under hypoosmotic conditions (Fig. 4 *a* and *b*).

The observed response time scale of B_2 GPCR is determined not only by the intrinsic reaction time scale of GPCR conformational change but also by the dependence of membrane tension on applied external mechanical perturbation. The relationship between applied fluid shear stress and membrane tension depends on a number of factors such as cell size, shape, cytoskeleton response, and the availability of an intracellular lipid pool. Active remodeling of the cytoskeleton and recruitment of intracellular lipids to the membrane can slow down the rate of increase in the membrane tension in response to a sudden mechanical stimulation of the cell. However, our experiments that probe the response of B2K to a sudden increase in membrane fluidity (Fig. 4 *c* and *d*) suggest that the intrinsic time constant of B2K conformational change is relatively slow, on the order of ≈180 s. In contrast, activation with a ligand at higher concentrations results in a conformational change after only 30 s (Fig. 1*d*). This finding is another indication that the equilibrium ternary complex model (26) may not be well suited for description of B2K conformational dynamics because the above data suggest that the ligand is not just binding to the active conformation but plays an active role in stimulating conformational transitions. Thus our data suggest that for B_2 receptor the "ligand induction" model is more appropriate; according to this model the free energy of ligand binding is used to overcame the conformational transition barrier to state R*. The response time to stimulation by shear stress is ≈80 s (Fig. 3*c*), which is faster than the response to the increase in membrane fluidity and means that membrane tension effect cannot be entirely attributed to an increase in membrane fluidity but must also lead to changes in other membrane properties (e.g., membrane thickness or increase in level of hydration).

Note that vastly varying ligand-induced switching times (from milliseconds to hundreds of seconds) have been reported for a few different classes of GPCRs and attributed to their different intended biological functions (13, 36); we believe that the relatively long switching time of B2K is similarly determined by its biological function. To our knowledge, no other study has reported the ligand-independent intrinsic GPCR activation rates. We believe that the measurements of GPCR conformational dynamics in response to perturbation of membrane microenvironment offer a unique approach for investigating intrinsic GPCR isomerization dynamics not easily accessible with other methods; in this case conformational dynamics of the GPCR itself is not masked by random ligand binding events.

Quantitative analysis of the presented FRET data shows that the magnitudes of the FRET ratio change caused by different membrane perturbations were as follows: ligand, 41%; shear stress, 8%; hypotonic stress, 13%; and benzyl alcohol, 5%. The relative number of responding receptors can be estimated by comparing the FRET ratio data for different perturbations to the FRET ratio changes caused by exposure to bradykinin at saturating concentration. Assuming that stimulation by a saturating concentration of the ligand activates 100% of receptors, a simple calculation indicates that the shear stress, hyptonic stress, and benzyl alcohol are responsible for conformational transitions in ≈14%, ≈23%, and ≈9% of all receptors, respectively.

The involvement of B_2 receptor in a flow-dependent response was demonstrated earlier by a number of studies reviewed elsewhere (17, 18, 41); impaired flow-dependent response was observed in arteries from knockout mice lacking B_2 receptors (17). Because the flow-dependent dilation is a fundamental mechanism by which large arteries ensure adequate supply of blood to the tissues (42, 43), our observation that the B_2 receptor can respond to mechanical perturbation of cell membrane without involvement of ligand suggests a molecular mechanism by which fluid shear stress can be sensed.

In summary, we have shown that fluid shear stress, hypoosmotic stimulation, and an increase in the plasma membrane fluidity lead to ligand-independent conformational transitions in B_2 GPCR in endothelial cells. We have also established the intrinsic time scale of GPCR conformational transitions in response to perturbation of the membrane microenvironment.

Methods

Time-Resolved Fluorescence Measurements. Time-resolved fluorescence emission kinetics and spectra were measured by using a multichannel, time-correlated single photon counting spectrograph (PML-16/SPC630; Becker & Hickl, Berlin, Germany) coupled to an inverted microscope (Axiovert 200 M; Zeiss, Thornwood, NY) via fiber optic link. A femtosecond Ti:Sapphire oscillator (Spectra-Physics, Irvine, CA) was used as the excitation source. The repetition frequency of the light pulses from the oscillator was reduced to 8 MHz, and the light wavelength was doubled to 435 nm and coupled into the microscope. The excitation light (≈0.1 μW) was defocused to a spot size of 20–50 μm to enable spatially homogenous excitation of a single cell. A dichroic beamsplitter (455dclp; Chroma, Rockingham, VT) was used to separate excitation from fluorescence light. Our experimental setup enabled detection of fluorescent transients from single cells with 16 independent wavelength channels and ≈20-ps time resolution. The photobleaching was ≈10% after 60-min illumination; it did not result in any noticeable changes of fluorescence spectra and kinetics on the time scale of our experiments. Fluorescence spectra were obtained by integrating time-resolved fluorescence data. The polarization of the detected fluorescence emission was selected by using polarizer. Most of the presented data (unless specified otherwise) were measured by detecting fluorescence emission polarized at 90° to the polarization of the excitation light at 435 nm, which enabled us to significantly increase sensitivity of our measurements because YFP emission is depolarized by the FRET process, whereas directly excited CFP and YFP emissions are polarized, resulting in lower overall background signal (see also ref. 23). The isotropic fluorescence emission kinetics were measured under the magic angle condition (54.7° angle between excitation and detection polarizations). The accuracy of anisotropy measurements was tested by measuring anisotropy of a model CFP–YFP pair (fluorescing proteins linked by a short, 11-residue

peptide), which exhibited cytoplasmic localization when expressed in BAECs; we found that the initial anisotropy value of CFP emission was ≈0.3, which is the same as reported in earlier studies (44).

Fluid Shear Stress Experiments. The fluid-induced shear stress studies were performed by using a parallel flow microchamber that allows exposure of endothelial cells to fluid shear stress up to 300 dynes/cm^2 in a flow channel (2 mm wide) that is optically accessible through a coverslip-based window; cells were imaged through high NA water immersion objective (C-Apochromat ×40/1.2). The design of the microchamber ensured that there was no deformation of glass coverslip (axial displacement was <0.05 μm) caused by flow-induced hydrostatic pressure. PBS was used as the perfusing medium. It has been shown that remodeling of the cytoskeleton of endothelial cells under fluid shear stress leads to significant cell shape changes only after prolonged stimulation for multiple hours (22, 45). We have detected no changes in cell shape (within resolution of our microscope system, ≈0.4 μm) irrespective of the type of stimulation (shear stress, benzyl alcohol, or hypoosmotic stress) on the time scale of our experiments.

Time-Resolved Data Analysis. Time-resolved fluorescence data were analyzed by using Globals Unlimited fluorescence data analysis software (University of Illinois, Urbana–Champaign, IL), which allowed fitting multiple fluorescence decays with multiexponential kinetic models to produce fluorescence lifetimes and ultimately FRET efficiencies. Each experiment was repeated on three to six cells, and the data were analyzed in paired fashion comparing relative change in signal from control cells to experimental preparations as needed.

DNA Constructs and Recombinant Proteins. cDNA templates of enhanced CFP (ECFP), enhanced YFP (EYFP), and human bradykinin B_2 type receptor were obtained from Invitrogen (Carlsbad, CA), Clontech (Mountain View, CA), and the University of Missouri cDNA Resource Center (Rolla, MO), respectively. Expression vector pECFP-N1 was purchased from Clontech. DNA primers for PCR amplifications were from Proligo, a Sigma (St. Louis, MO) company. A primer extension method was used to construct B2K by inserting EYFP into the third cytoplasmic loop at a position between F232 and K233 and fusing ECFP to the truncated C terminus at the position C329. The DNA fragment of B2K, with EYFP inserted between the two codons encoding residues F232 and K233, was constructed by two steps of PCR primer extension using the following oligos: 5′-ATGCAGAAGTTCGTGAGCAAGGGCGAGGAG-3′ and 5′-GCCCTTGCTCACGAACTTCTGCATCTCGTT-3′ for linking of EYFP N terminus to B2K, and 5′-GAGCTGTACAAGAAGGAGATCCAGACGGAG-3′ and 5′-CTGGATCTCCTTCTTGTACAGCTCGTCCAT-3′ for linking of EYFP C terminus to B2K. Oligos 5′-GCTAGCGTTTAAACTTAAGCTTGGT-3′ (complementary to pcDNA3.1hygro expression vector encoding B2K) and 5′-CGACCGGTGCGCCCCCTTTCTGGCACACTC-3′ were used for cloning of the DNA fragment into HindIII and Age1 sites of pECFP-N1, fusing the fragment in-frame to ECFP.

Cell Culture and Protein Expression. BAECs (passages 2–6; Cambrex, East Rutherford, NJ) were cultured on microscope coverslips in DMEM supplemented with 10% FBS and antibiotics and maintained in a humidified 5% CO_2–95% air incubator at 37°C. BAEC transfection was done by using Targeting System (Santee, CA) reagent Targefect-2 and Virofect enhancer. HEK293 cells were cultured in DMEM and used only for long-lasting experiments (dose–response measurements) when sufficient transfection efficiency could not be achieved in BAECs.

We thank all researchers at the La Jolla Bioengineering Institute for helpful discussions. This research was supported in part by National Institutes of Health Grant HL40696.

1. Sukharev SI, Blount P, Martinac B, Blattner FR, Kung C (1994) *Nature* 368:265–268.
2. Paoletti P, Ascher P (1994) *Neuron* 13:645–655.
3. Gudi S, Nolan JP, Frangos JA (1998) *Proc Natl Acad Sci USA* 95:2515–2519.
4. Lehtonen JYA, Kinnunen PKJ (1995) *Biophys J* 68:1888–1894.
5. Knudsen HL, Frangos JA (1997) *Am J Physiol* 42:H347–H355.
6. Lee AG (2004) *Biochim Biophys Acta* 1666:62–87.
7. Zou YZ, Akazawa H, Qin YJ, Sano M, Takano H, Minamino T, Makita N, Iwanaga K, Zhu WD, Kudoh S, *et al.* (2004) *Nat Cell Biol* 6:499–506.
8. Sadoshima J, Xu Y, Slayter HS, Izumo S (1993) *Cell* 75:977–984.
9. Gether U (2000) *Endocr Rev* 21:90–113.
10. Farrens DL, Altenbach C, Yang K, Hubbell WL, Khorana HG (1996) *Science* 274:768–770.
11. Ghanouni P, Gryczynski Z, Steenhuis JJ, Lee TW, Farrens DL, Lakowicz JR, Kobilka BK (2001) *J Biol Chem* 276:24433–24436.
12. Vilardaga JP, Steinmeyer R, Harms GS, Lohse MJ (2005) *Nat Chem Biol* 1:25–28.
13. Vilardaga JP, Bunemann M, Krasel C, Castro M, Lohse MJ (2003) *Nat Biotechnol* 21:807–812.
14. Hoffmann C, Gaietta G, Bunemann M, Adams SR, Oberdorff-Maass S, Behr B, Vilardaga JP, Tsien RY, Eisman MH, Lohse MJ (2005) *Nat Methods* 2:171–176.
15. Perez DM, Karnik SS (2005) *Pharmacol Rev* 57:147–161.
16. Leeb-Lundberg LMF, Marceau F, Muller-Esterl W, Pettibone DJ, Zuraw BL (2005) *Pharmacol Rev* 57:27–77.
17. Bergaya S, Meneton P, Bloch-Faure M, Mathieu E, Alhenc-Gelas F, Levy BI, Boulanger CM (2001) *Circ Res* 88:593–599.
18. Groves P, Kurz S, Just H, Drexler H (1995) *Circulation* 92:3424–3430.
19. Hess JF, Borkowski JA, MacNeil T, Stonesifer GY, Fraher J, Strader CD, Ransom RW (1994) *Mol Pharmacol* 45:1–8.
20. Fathy DB, Leeb T, Mathis SA, Leeb-Lundberg LM (1999) *J Biol Chem* 274:29603–29606.
21. Paquet JL, Luccarini JM, Fouchet C, Defrene E, Loillier B, Robert C, Belichard P, Cremers B, Pruneau D (1999) *Br J Pharmacol* 126:1083–1090.
22. Barbee KA, Davies PF, Lal R (1994) *Circ Res* 74:163–171.
23. Rizzo MA, Piston DW (2005) *Biophys J* 88:L14–L16.
24. Haidekker MA, Ling TT, Anglo M, Stevens HY, Frangos JA, Theodorakis EA (2001) *Chem Biol* 8:123–131.
25. Kung CE, Reed JK (1986) *Biochemistry* 25:6114–6121.
26. Lefkowitz RJ, Cotecchia S, Samama P, Costa T (1993) *Trends Pharmacol Sci* 14:303–307.
27. Roberts DJ, Waelbroeck M (2004) *Biochem Pharmacol* 68:799–806.
28. Shea LD, Neubig RR, Linderman JJ (2000) *Life Sci* 68:647–658.
29. Gullingsrud J, Schulten K (2004) *Biophys J* 86:3496–3509.
30. Needham D, Nunn RS (1990) *Biophys J* 58:997–1009.
31. Blood PD, Ayton GS, Voth GA (2005) *J Phys Chem B* 109:18673–18679.
32. Martinac B, Hamill OP (2002) *Proc Natl Acad Sci USA* 99:4308–4312.
33. Botelho AV, Gibson NJ, Thurmond RL, Wang Y, Brown MF (2002) *Biochemistry* 41:6354–6368.
34. Wang Y, Botelho AV, Martinez GV, Brown MF (2002) *J Am Chem Soc* 124:7690–7701.
35. Gether U, Kobilka BK (1998) *J Biol Chem* 273:17979–17982.
36. Ghanouni P, Steenhuis JJ, Farrens DL, Kobilka BK (2001) *Proc Natl Acad Sci USA* 98:5997–6002.
37. Zhang YL, Frangos JA, Chachisvilis M (2006) *Biochem Biophys Res Commun* 347:838–841.
38. Butler PJ, Norwich G, Weinbaum S, Chien S (2001) *Am J Physiol* 280:C962–C969.
39. Hanggi P, Talkner P, Borkovec M (1990) *Rev Mod Phys* 62:251–341.
40. Borochov A, Borochov H (1979) *Biochim Biophys Acta* 550:546–549.
41. Skidgel RA, Alhenc-Gelas F, Campbell WB (2003) *Am J Physiol* 284:H1886–H1891.
42. Bevan JA, Kaley G, Rubanyi GM (1995) *Flow-Dependent Regulation of Vascular Function* (Oxford Univ Press, New York).
43. Davies PF (1995) *Physiol Rev* 75:519–560.
44. Rizzo MA, Springer GH, Granada B, Piston DW (2004) *Nat Biotechnol* 22:445–449.
45. Galbraith CG, Skalak R, Chien S (1998) *Cell Motil Cytoskeleton* 40:317–330.